AIP | The Journal of Chemical Physics

Seeding approach to crystal nucleation

Jorge R. Espinosa, Carlos Vega, Chantal Valeriani, and Eduardo Sanz

Citation: The Journal of Chemical Physics **144**, 034501 (2016); doi: 10.1063/1.4939641
View online: http://dx.doi.org/10.1063/1.4939641
View Table of Contents: http://scitation.aip.org/content/aip/journal/jcp/144/3?ver=pdfcov
Published by the AIP Publishing

Seeding approach to crystal nucleation

Jorge R. Espinosa,[1] Carlos Vega,[1] Chantal Valeriani,[1,2] and Eduardo Sanz[1]
[1]*Departamento de Quimica Fisica I, Facultad de Ciencias Quimicas, Universidad Complutense de Madrid, 28040 Madrid, Spain*
[2]*Departamento de Fisica Aplicada I, Facultad de Ciencias Fisicas, Universidad Complutense de Madrid, 28040 Madrid, Spain*

(Received 15 October 2015; accepted 24 December 2015; published online 21 January 2016)

We present a study of homogeneous crystal nucleation from metastable fluids via the seeding technique for four different systems: mW water, Tosi-Fumi NaCl, Lennard-Jones, and Hard Spheres. Combining simulations of spherical crystal seeds embedded in the metastable fluid with classical nucleation theory, we are able to successfully describe the nucleation rate for all systems in a wide range of metastability. The crystal-fluid interfacial free energy extrapolated to coexistence conditions is also in good agreement with direct calculations of such parameter. Our results show that seeding is a powerful technique to investigate crystal nucleation. © *2016 AIP Publishing LLC*. [http://dx.doi.org/10.1063/1.4939641]

I. INTRODUCTION

The transition between a liquid and a crystal is a phenomenon of great importance in areas as diverse as biology (e.g., protein crystallization), climate change (crystallization in clouds), industry (e.g., drugs production), geology, or optics. The emergence of a growing crystal nucleus in the fluid phase is the first step of the liquid-to-crystal transition.[1] The rate, size, and structure with which such nucleus appears are fundamental parameters for the understanding and control of crystallization.

Whereas the nucleation rate can be measured experimentally,[2–6] a microscopic description of the crystal nucleus remains elusive to current experimental techniques, due to the small size (∼nm) and short life (∼ns) of the nucleus.[7] To overcome this experimental shortcoming two different approaches are pursued. One is the use of colloidal systems as models for atomic and molecular systems.[8] Due to its big size (∼μm), colloids can be seen and tracked in a microscope.[9] However, despite significant advances in the synthesis of colloidal particles,[10] most investigations of crystal nucleation are restricted to spherical particles with isotropic interactions.[9,11]

An alternative approach to the study of the mechanism of crystal nucleation is the use of computer simulations[12] that provide a detailed description of the system at a molecular level.[13,14] The main problem faced by simulations is that, for moderately supercooled fluids, the emergence of a crystal nucleus is a rare event and cannot be directly probed in the size and time scales accessible to brute force molecular dynamics. Therefore, special rare event simulation methods like Umbrella Sampling (US),[15–29] Forward Flux Sampling (FFS),[20,21,29–33] metadynamics,[34,35] or transition path Sampling[14,36,37] have to be employed. Although these methods artificially accelerate the appearance of the crystal nucleus they do not, in principle, alter the true crystallization mechanism. However, the use of these methods is quite demanding computationally, which restricts most studies to deeply metastable fluids, where the critical cluster is small (about 100-200 particles).

An approximate simulation approach, which we refer to as "seeding," has been used in the last few years to study nucleation in conditions of shallow metastability.[38–44] The technique is based in seeding the fluid with a crystal cluster. The microscopic information of the critical cluster obtained by means of simulations is combined with Classical Nucleation Theory (CNT)[1,45,46] to get estimates of the nucleation rate. The seeding method is quite simple to implement and enables the estimation of the nucleation rate in a broad range of orders of magnitude.[41–43] However, the method is approximate because it relies on the validity of both an *a priori* conceived nucleation pathway (the one going through the inserted seed) and of classical nucleation theory. It is therefore important to assess the extent to which this powerful but approximate technique can be confidently used.

The first seeding simulations were not so encouraging in this respect, as they provided a value of the crystal-fluid interfacial free energy, γ, for the Lennard-Jones (LJ) system of $0.30\,\epsilon/\sigma^2$,[38] that does not quite agree with values ranging from 0.35 to $0.37\,\epsilon/\sigma^2$ obtained in direct calculations[47–50] (where ϵ and σ are the energy and length scales of the Lennard-Jones system, respectively). Later on, the seeding method was used to estimate the nucleation rate of chlatrates,[39] but the results were not compared against rigorous calculations. We have used the seeding technique to investigate homogeneous ice nucleation and realised that an extrapolation of our results for the mW model to high supercooling gives reasonable, although not entirely satisfactory, results.[42] We have also recently studied NaCl,[43] for which seeding seems to work particularly well. Very recently, the seeding technique has been even applied to crystal nucleation from solution[44] but, again, a quantitative comparison with rigorous techniques has not been performed. In summary, the ability of the seeding

method to quantitatively predict crystal nucleation rates still remains unclear.

In this work we assess the validity of the seeding approach by comparing the nucleation rate and the interfacial free energy obtained by seeding to those calculated using more rigorous methods. We use four different models for that purpose: mW water, Tosi-Fumi (T-F) NaCl, Lennard Jones, and Hard Spheres (HS). We conclude that the seeding method is successful in all the cases within the accuracy of the calculations.

II. MODELS AND SIMULATION DETAILS

We use four different models to test the ability of the seeding technique to predict nucleation rates.

One is the mW water model.[51] All simulations for this model are performed at 1 bar. The melting temperature of the mW model at 1 bar is 274.6 K.[51] We use the LAMMPS package[52] to perform molecular dynamics simulations of mW water. Further details on our simulations of this system can be found in Ref. 42. Although we have already reported seeding results for the mW model in Ref. 42 here we revisit and refine our previous calculations (see Discussion below).

We also study the truncated and shifted LJ potential in the form proposed by Broughton and Gilmer.[53] The depth of the interaction potential, ϵ, and the distance at which the interaction potential is zero, σ, are used as energy and distance units, respectively. All simulations are performed at pressure $-0.02\epsilon/\sigma^3$, for which the melting temperature is $T = 0.617\epsilon/k_B$.[47] We use the GROMACS[54] implementation for Ar to simulate the LJ system, with $\sigma = 3.405$ Å, $\epsilon = 0.997$ KJ/mol, and atomic mass of 6.69×10^{-26} kg. The time unit for the LJ system is defined as $\tau = ((m\sigma^2)/(\epsilon))^{1/2}$. Pair interactions are truncated at 8.5 Å.

Moreover, we investigate the HS model. For practical reasons, we use the continuous version of the HS potential proposed in Ref. 55. This potential has been shown to closely reproduce the equation of state,[55] dynamics,[55] phase diagram,[56] and crystal-fluid interfacial free energy[48] of pure HS. In this work, we show that the continuous model also reproduces the nucleation rate of pure HS. We use the same simulation details as in Refs. 48 and 56. To report quantities pertaining to this system, we use the particle diameter, σ, as unit of length and as unit of time $\sigma^2/(6D_l)$, where D_l is the self diffusion coefficient of the fluid. Pair interactions are truncated at 1.175 σ.

Finally, we also discuss for completeness the case of crystallization of the T-F model[57,58] of NaCl at 1 bar, which we recently published in Ref. 43. For this model, the melting temperature at 1 bar is 1082 K.[59] Further details on the simulations of this system are given in Ref. 43. We use particle mesh Ewald summations[60] to deal with electrostatic interactions. The cutoff radius for dispersive interactions and for the real part of electrostatic interactions is 14 Å.

In the molecular dynamics simulations carried out in GROMACS (for the LJ, NaCl and (pseudo)HS systems) pressure is kept constant using an isotropic Parrinello-Rahman barostat[61] with a relaxation time of 0.5 ps. To fix the temperature we employ a velocity-rescale thermostat[62] with a relaxation time of 0.5 ps. The time step for the Verlet integration of the equations of motion is 2 fs in all cases. In the simulations for the mW model, carried out with the LAMMPS package, temperature is kept constant with the Nose-Hoover thermostat[63] and pressure with the Nose-Hoover barostat,[64] implemented as described in Ref. 65. The relaxation time for both the thermostat and the barostat is 0.5 ps. The time step for the integration of the equations of motion is 5 fs.

III. THE SEEDING METHOD

According to CNT, the appearance of a crystal cluster in a metastable fluid entails a Gibbs free energy change, ΔG given by

$$\Delta G(N) = -N|\Delta\mu| + \gamma A, \tag{1}$$

where N is the number of particles in the crystal cluster, $|\Delta\mu|$ is the chemical potential difference between the fluid and the crystal, A is the area of the cluster's surface, and γ is the crystal-fluid interfacial free energy. The two competing terms in the expression above give rise to a free energy barrier whose top corresponds to a cluster of critical size N_c. By maximizing Eq. (1) with respect to N, one gets the height of the free energy barrier,

$$\Delta G_c = N_c|\Delta\mu|/2 \tag{2}$$

and assuming a spherical cluster shape, a critical cluster size of

$$N_c = \frac{32\pi\gamma^3}{3\rho_s^2|\Delta\mu|^3}, \tag{3}$$

where ρ_s is the density of the solid cluster.

The number density of critical clusters is given by $\rho_f \exp[-\Delta G_c/(k_BT)]$ (where ρ_f is the density of the fluid). Such density, multiplied by a kinetic pre-factor, gives the following CNT expression for the nucleation rate, J,

$$J = \sqrt{\frac{|\Delta\mu|}{6\pi k_BTN_c}} f^+\rho_f \exp[-\Delta G_c/(k_BT)], \tag{4}$$

where f^+ is the attachment rate of particles to the critical cluster.

TABLE I. Values of the variables leading to the calculation of J for mW water via the seeding technique. See main text for the meaning of each variable.

N_c	N_T	ΔT_c/K	$\lvert\Delta\mu\rvert$/(kcal/mol)	ρ_f/(g/cm^3)	γ/(mJ/m^2)	$(f^+/10^{14})$/(s^{-1})	λ/Å	$\Delta G_c/(k_BT)$	$\log_{10}$(J m^3 s)
688	22 956	34.6	0.155	1.0040	30.4	0.7	2.51	112	−9
1916	77 585	24.6	0.112	1.0037	30.7	1.9	2.38	216	−54
3202	77 585	22.1	0.101	1.0035	32.7	2.5	2.54	321	−99
7247	183 994	17.1	0.0783	1.0033	33.0	4.9	2.52	555	−201

TABLE II. Values of the variables leading to the calculation of J for LJ via the seeding technique. See main text for the meaning of each variable.

N_c	N_T	$T_c/(\epsilon/k_B)$	$\rho_f/(\sigma^{-3})$	$\lvert\Delta\mu\rvert/(k_BT)$	$\gamma/(\epsilon/\sigma^2)$	f^+/τ	λ/σ	$\Delta G_c/(k_BT)$	$\log_{10}(J\sigma^3\tau)$
585	31 901	0.534	0.868	0.246	0.33	40	1.15	72	−32
3 794	87 665	0.572	0.851	0.127	0.342	512	0.73	242	−106
12 672	275 758	0.587	0.843	0.084	0.348	650	1.00	533	−234

By inserting Eq. (2) in Eq. (4), it becomes evident that the four factors needed to obtain an estimate of J at a certain T are N_c, ρ_f, $|\Delta\mu|$, and f^+.

The evaluation of N_c is what gives the name "seeding" to the technique. It consists in inserting a cluster of a given shape with a given structure in the supercooled fluid. The way this configuration is prepared is described in detail in Ref. 43. Starting from such configuration, we monitor the number of particles in the cluster for different temperatures. If the temperature is higher than that makes the inserted cluster critical, the cluster will melt, and viceversa. In such way one can identify the temperature T_c for which the inserted cluster is critical as that enclosed between the highest temperature at which the cluster grows and the lowest at which it melts. We have used this method to determine the critical size of ice[41,42] and NaCl clusters.[43] In Section IV, we show an example of the determination of a critical cluster size and discuss the way we determine the number of particles belonging to the crystal cluster. The latter is a crucial point in the seeding technique given that N_c directly affects the calculation of both the nucleation rate and the interfacial free energy.

In this work, we consider spherical clusters with the structure of the equilibrium crystal phase for all investigated systems. In previous work, we considered the possibility that clusters of NaCl and cubic ice (both structures with cubic unit cells) have a cubic shape, but we concluded that they are better represented by a sphere[43,66] (of course, the surface of the cluster is not smooth but is roughened by capillary fluctuations intrinsic to the crystal-fluid interface[67,68]). In what follows, we show that spherical clusters do indeed a good job in the prediction of crystal nucleation rates for water, Lennard-Jones, NaCl, and HS.

The density of the fluid ρ_f is trivially calculated from an ensemble average in an NpT simulation at the temperature at which the cluster is found to be critical. $|\Delta\mu|$ can be computed either by direct calculations of the chemical potential of the fluid and crystal phases like in Ref. 66, or by thermodynamic integration from the melting temperature as described in Ref. 42.

To obtain f^+, we follow the expression proposed by Auer and Frenkel,[18,69]

$$f^+ = \frac{\langle (N(t) - N_c)^2 \rangle}{2t}. \tag{5}$$

Computing f^+ requires monitoring the number of particles in the cluster, N, for several trajectories launched at the temperature at which the cluster is critical. We show this type of trajectories for NaCl and for water in Refs. 43, 41, and 42, respectively.

After having calculated N_c, ρ_f, $|\Delta\mu|$, and f^+, a value of J is derived from Eq. (4). This procedure is repeated for 3 or 4 different cluster sizes typically ranging from $\sim 10^3$ to $\sim 10^4$ molecules. In such way we have 3-4 (J,T) points at low supercoolings where the calculations with rigorous rare event techniques would be too demanding.

Once the nucleation rate is obtained for a few points, one can try to fit them with a CNT expression in order to get a $J(T)$ curve that can be extrapolated outside the temperature range where the seeding calculations were performed. This entails obtaining N_c, ρ_f, $|\Delta\mu|$, and f^+ as a function of temperature.

Directly fitting the obtained N_c's as a function of temperature is not a good choice because the critical size sharply drops in a non-linear fashion as the temperature decreases, so it is not possible to describe $N_c(T)$ with only 3 or 4 points. Instead, we use Eq. (3) to obtain γ for each simulated cluster. By contrast to $N_c(T)$, we find that $\gamma(T)$ is a smooth function (linear for both NaCl and water[41–43]). Once $\gamma(T)$ is known, we obtain $N_c(T)$ via Eq. (3).

In order to obtain $\rho_f(T)$ we simply perform NpT simulations of the fluid at several temperatures and fit the average density as a function of temperature to the simplest possible functional form (typically a second order polynomial function suffices). Regarding $|\Delta\mu|$, it can be obtained in a straightforward manner by integrating the enthalpy difference between the crystal and the fluid from the melting temperature as shown in Ref. 42.

TABLE III. Values of the variables leading to the calculation of J for HS via the seeding technique. See main text for the meaning of each variable.

N_c	N_T	$p/((k_BT)/\sigma^3)$	$\lvert\Delta\mu\rvert/(k_BT)$	ϕ	$\gamma/(k_BT/\sigma^2)$	$f^+/(6D_l/\sigma^2)$	λ/σ	$\Delta G_c(k_BT)$	$\log_{10}[J/(6D_l/\sigma^5)]$
340	6 819	14.5	0.285	0.518	0.658	1 850	0.38	48	−19.5
547	23 145	14.286	0.263	0.516	0.70	2 110	0.36	70	−29
1 075	23 145	13.581	0.193	0.511	0.65	4 294	0.31	104	−44
3 814	107 763	12.861	0.122	0.505	0.62	12 397	0.28	232	−100
9 066	202 461	12.559	0.0914	0.502	0.61	39 584	0.21	414	−178
39 029	865 074	12.220	0.0567	0.499	0.609	112 120	0.20	1107	−479

Finally, to obtain $f^+(T)$, we use the following CNT expression for f^+:

$$f^+(T) = \frac{24D(T)[N_c(T)]^{2/3}}{\lambda^2}, \quad (6)$$

where D is the diffusion coefficient of the liquid and λ is the distance travelled by particles in the vicinity of the cluster to attach to the cluster's surface. $D(T)$ is obtained by fitting the diffusion coefficient of the fluid obtained in NpT molecular dynamics simulations at several temperatures. $N_c(T)$ is obtained through $\gamma(T)$ as explained in the previous paragraphs. For a given temperature, λ is obtained by equating Eq. (6) to the value of f^+ obtained via Eq. (5). As shown in Tables I–III the value of λ thus calculated does not change much with temperature and takes values of the order of the molecular diameter. To obtain $f^+(T)$ via Eq. (6), we use λ averaged over all studied temperatures for a given model.

With N_c, ρ_f, $|\Delta\mu|$, and f^+ as a function of temperature, we obtain $J(T)$ via Eq. (4). For the HS system, it is not the temperature, but the pressure that controls the freezing transition. Therefore, the same procedure is followed using pressure instead of temperature as independent variable.

IV. NUMBER OF PARTICLES IN THE CLUSTER

To determine the critical cluster size, we look for the temperature that makes a given cluster size critical. In Fig. 1, we show the trajectories that are used to determine the temperature at which an ice cluster of 3202 mW molecules is critical. In view of the trajectories shown in Fig. 1, we conclude that the inserted cluster is critical at a temperature $T_c = 252.5 \pm 2.5$ K.

In order to monitor the number of particles in the crystal cluster, we need to label particles as liquid- or solid-like. This is done by evaluating for each particle a function (order parameter) sensitive to the degree of local order.[17,70] The threshold in the order parameter for labelling a particle either as liquid or as solid is chosen in such way that the probability of mislabelling particles in the bulk liquid as solid-like is the same as that of mislabelling particles in the bulk solid as liquid-like. The chosen order parameter is the one that gives the lowest mislabelling probability.

To illustrate this procedure, we follow on with the example of mW water. In Fig. 2(a), we show $(\bar{q}_4,\bar{q}_6)$ points for molecules in the bulk ice-Ih and liquid phases at T = 254 K. For the calculation of the $\bar{q}_i$ order parameter, we follow Ref. 70. As it is evident from Fig. 2(a), the $\bar{q}_6$ order parameter is able to discriminate between liquid and solid molecules, whereas the $\bar{q}_4$ is not. In Fig. 2(b), we plot the percentage of mislabelled

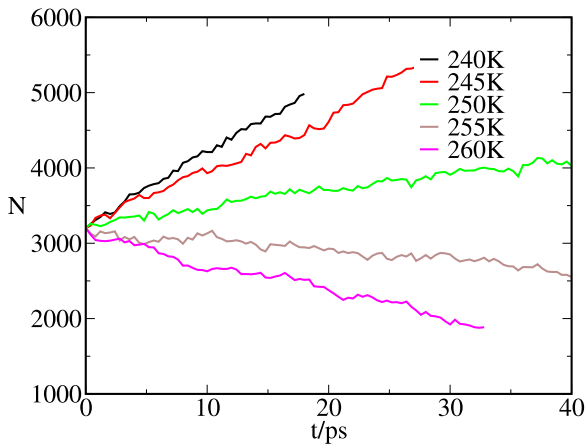

FIG. 1. Number of particles in the cluster versus time for mW water at several temperatures (see legend) and 1 bar starting from a configuration with a cluster containing 3202 molecules.

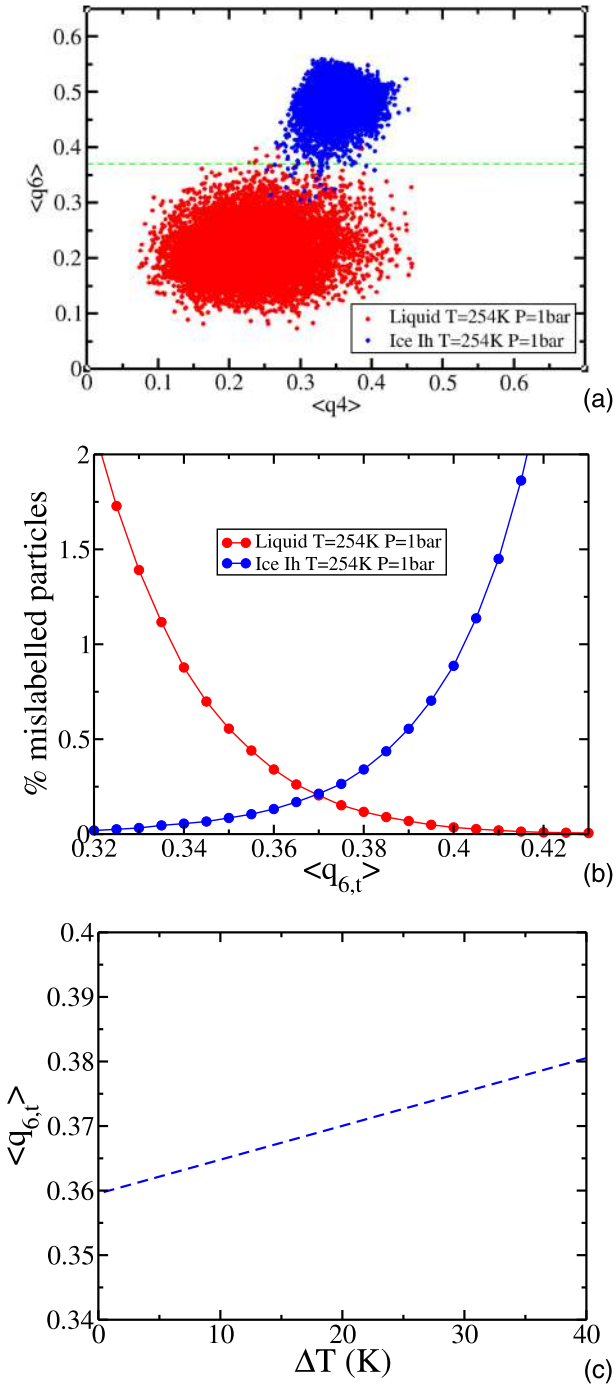

FIG. 2. Procedure to distinguish liquid from solid-like molecules for mW water. (a) $\bar{q}_6$ versus $\bar{q}_4$ for 10 000 liquid (red) and 10 000 ice-Ih (blue) bulk molecules at 254 K. (b) Percentage of mislabelled bulk particles for each phase as a function of $\bar{q}_{6,t}$ at 254 K. (c) Dependence of the optimal $\bar{q}_{6,t}$ on the supercooling.

bulk particles as a function of the threshold chosen for the $\bar{q}_6$ order parameter, $\bar{q}_{6,t}$. The crossing point between the mislabelling curves of the liquid and solid phases gives the optimal value for $\bar{q}_{6,t}$ at T = 254 K. The optimal threshold smoothly changes with temperature, as shown in Fig. 2(c). This means that, in principle, one should use a different $\bar{q}_{6,t}$ for each temperature. This is the procedure we follow for the mW model. For this model, the cut-off for both computing $\bar{q}_{6,t}$ and identifying the biggest cluster has been 3.51 Å. For the LJ (HS) model $\bar{q}_{6,t}$ changes little with temperature (pressure) and we have simply used the average $\bar{q}_{6,t}$ in the range of studied temperatures (pressures). The thresholds used for the LJ and HS models are $\bar{q}_{6,t} = 0.362$ and $\bar{q}_{6,t} = 0.372$, respectively. The cut-off for LJ (HS) for both computing $\bar{q}_{6,t}$ and identifying the biggest cluster has been 1.432σ (1.33σ). For the T-F NaCl model, we use the order parameter described in Ref. 20 to distinguish liquid from solid-like particles.

V. NUCLEATION RATE

In Tables I–III, we report all variables leading to the calculation of the nucleation rate for mW water, LJ, and HS, respectively. With ΔT_c, we refer to the supercooling corresponding to a given cluster, where the supercooling is defined as the difference between the melting temperature and the temperature of interest. For HS and LJ, we report $|\Delta\mu|$ in k_BT per particle. We also report the total number of particles in the simulation box, N_T. The values for T-F NaCl are reported in Ref. 43.

In Fig. 3, we show the decimal logarithm of the nucleation rate as a function of the supercooling for mW water, T-F NaCl, and LJ, and as a function of the volume fraction occupied by spheres, $\phi = \pi/6\rho_f\sigma^3$, for HS. With symbols, we show our seeding calculations (black circles) alongside calculations from other techniques as indicated in the legend. The seeding technique enables the estimation of the nucleation rate at lower supercooling than any other technique. The technique that requires the largest supercooling is obviously "brute force," where nucleation takes place in the course of a standard NpT molecular dynamics simulation. Also note that with the seeding technique one can estimate the rate in a wide range of orders of magnitude, whereas more rigorous methods are restricted to a narrower window because they are more demanding from a computational point of view. However, the seeding is an approximate method and has to be validated by comparing it against rigorous approaches. For the case of mW,

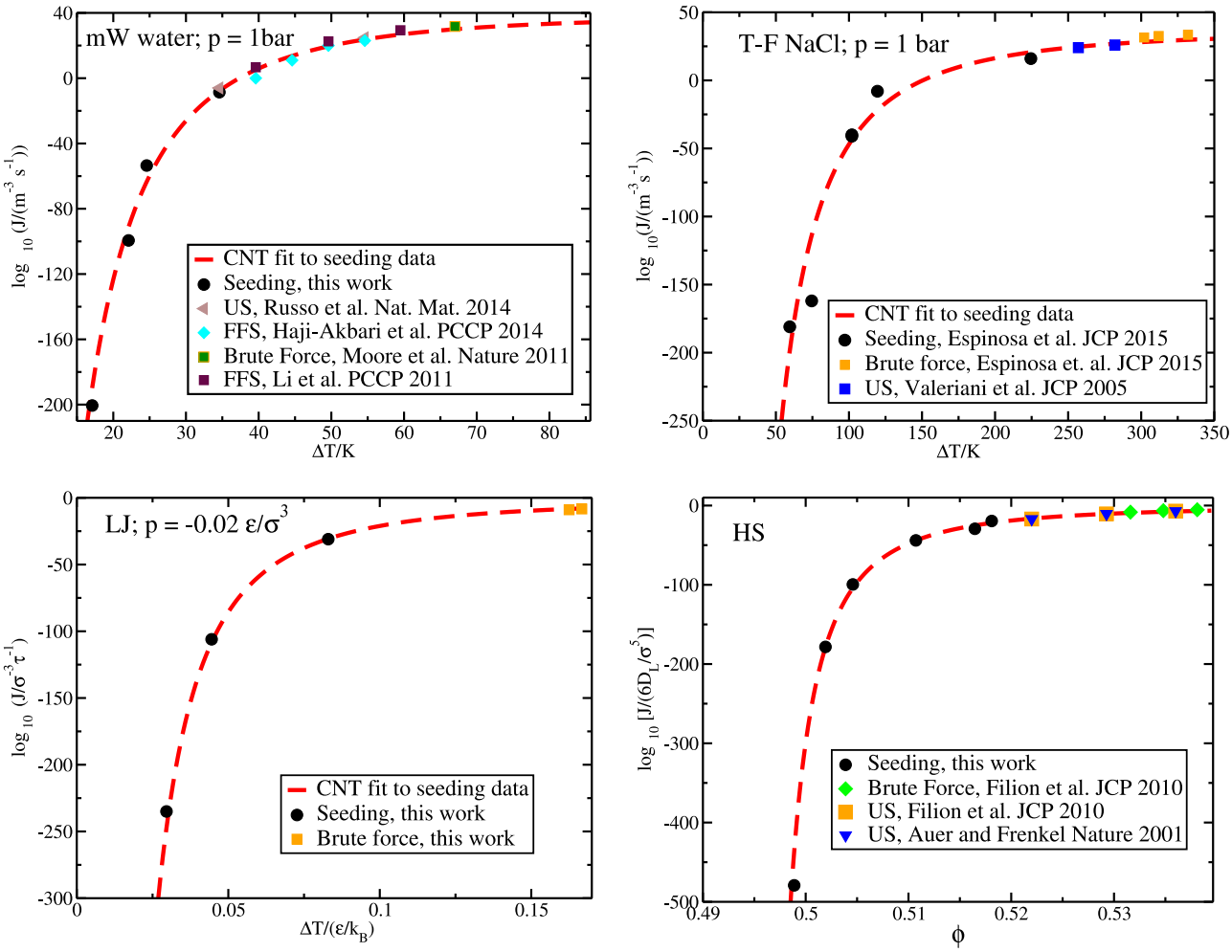

FIG. 3. Top-left, top-right, and bottom-left: logarithm of the nucleation rate as a function of the supercooling for the mW water model, the T-F NaCl model, and the LJ model, respectively. Bottom-right: logarithm of the nucleation rate as a function of the volume fraction of the parent fluid phase for the HS model. Symbols and curves as indicated in the legend.

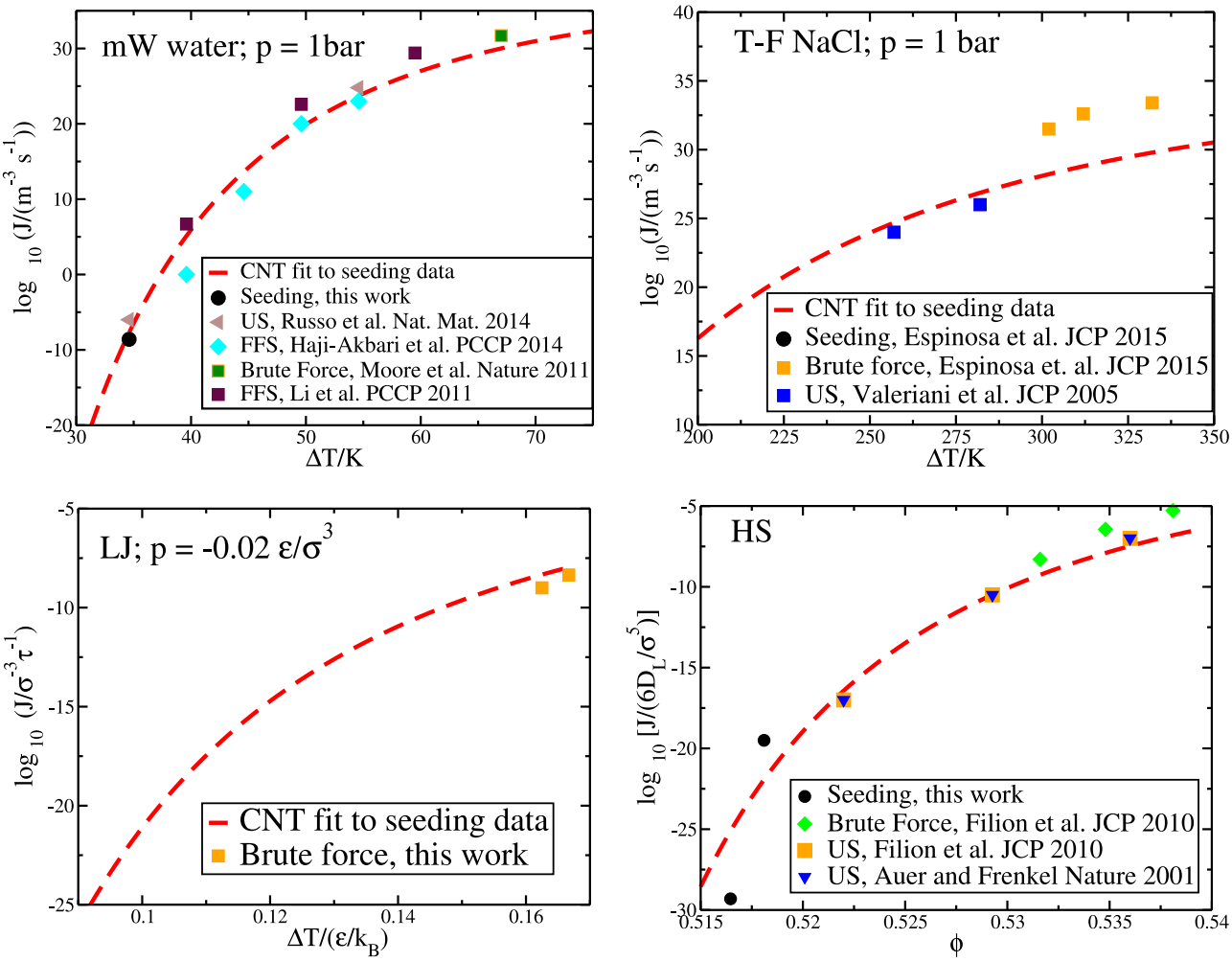

FIG. 4. Zoom of the plots shown in Fig. 3 for the region where a comparison is established with literature data and our own brute force simulations for the LJ system.

there is one point for which we can make this comparison: for a supercooling of 34.5 K seeding and US[24] are in good agreement, which is quite encouraging.

To further test the ability of the seeding scheme to predict nucleation rates, we fit our data with a CNT expression (see Sec. III) and extrapolate our results to high supercooling, where we have a wealth of data from rigorous simulations to compare to. Such fits are shown by red dashed lines in Fig. 3. In all four systems the agreement between the CNT fit and more rigorous calculations is very good. Within 4 orders of magnitude (which is roughly the uncertainty of the fit) the CNT fit to the seeding data agrees with the calculations by Russo *et al.*,[24] Haji-Akbari and Debenedetti,[33] Moore and Molinero,[71] and Li *et al.*[32] for the mW water model; by Valeriani *et al.*[20] and Espinosa *et al.*[43] for the T-F NaCl model; by Auer and Frenkel,[18] and Filion *et al.*[21] for HS; and with our own brute force calculations for LJ. A zoom of Fig. 3 in the region where we compare the CNT fit to other data is shown in Fig. 4. Notice in Fig. 4 that for the mW model at $\Delta T = 39.5$ K there are two conflicting the literature data. Both have been obtained with the FFS technique and differ by more than 6 orders of magnitude.[32,33] We are uncertain about the origin of this discrepancy, but the value obtained from seeding is closer to that of Li *et al.*

VI. INTERFACIAL FREE ENERGY

Using Eq. (3), we can obtain the interfacial free energy for each inserted cluster. Our seeding results are shown as black dots in Fig. 5 for the four studied models. By linearly fitting our data, we can extrapolate γ to coexistence conditions, where we can compare to direct calculations of γ for a flat interface by contrasted methods like capillary wave fluctuations (CF),[72] cleaving (CL),[73] or mold integration.[48] When performing such comparison one should take into account that direct calculations provide γ for specific crystal orientations, whereas the γ obtained from spherical clusters is an average for all crystal orientations. Nevertheless, both approaches should yield similar values, as is the case for all four systems investigated. In fact, the γ extrapolated at coexistence from the seeding data is consistent with direct calculations by Limmer and Chandler[74] for mW water; by Espinosa *et al.*[43] for T-F NaCl; by Davidchack and Laird,[47] Espinosa *et al.*,[48] Agioletti-Uberti *et al.*,[49] Morris and Song,[75] and Benjamin and Horbach[50] for LJ; and by Davidchack and Laird,[76,77] Espinosa *et al.*,[48] Benjamin and Horbach,[78] and Hartel *et al.*[79] for HS. Note that for the sake of clarity we have not included in Fig. 5 all data available in the literature. In summary, the seeding method is able to yield good estimates

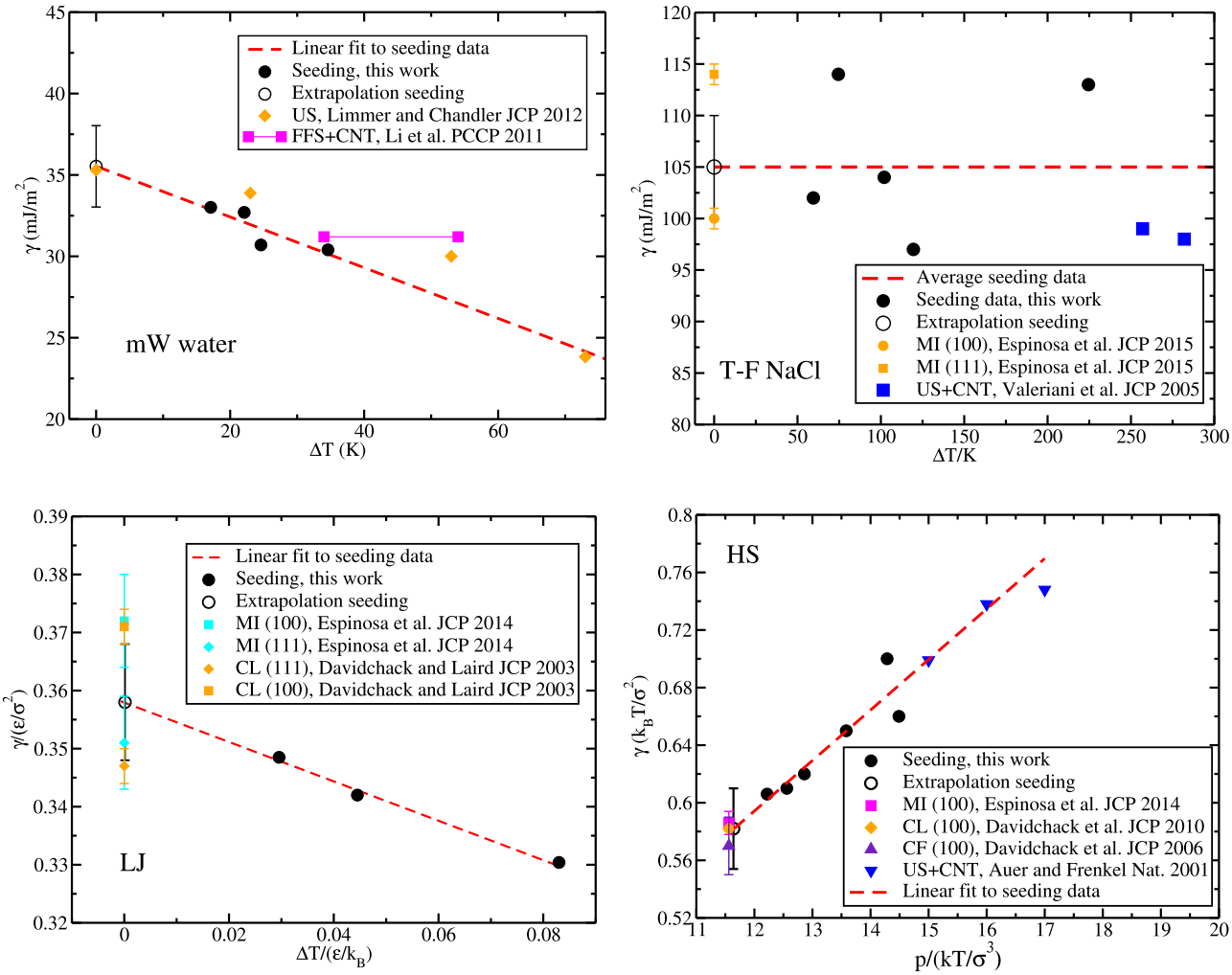

FIG. 5. Crystal-melt interfacial free energy as a function of the supercooling/pressure. Top left, mW water model; top right, T-F NaCl model; bottom left, LJ model; bottom right, HS model. Symbols and dashed lines as indicated in the legend.

of the crystal-fluid interfacial free energy at coexistence for all studied systems. We summarize the values of γ at coexistence from our seeding simulations in Table IV.

In Fig. 5, we also compare our seeding results with the literature data for conditions of metastability (below the melting temperature for mW water, T-F NaCl, and LJ, or above the coexistence pressure for HS). The only direct calculations of γ at such conditions that do not rely on CNT are those of Limmer and Chandler for mW water.[74] Their data are in reasonable agreement with ours. The other data available depend on CNT and can only be directly compared to ours if the same criterion to measure the size of the crystal nucleus is employed. This is the case only for T-F NaCl, for which we have a good agreement with the US simulations by Valeriani *et al.*[20] For mW water and for HS, we have a reasonable agreement with Li *et al.*[32] and Auer and Frenkel,[18] although, as already mentioned, in these cases any discrepancy could be due to differences in the criterion with which the size of the cluster is determined.

TABLE IV. Interfacial free energy extrapolated to the equilibrium coexistence conditions (planar interface) from seeding calculations.

Model	γ
mW water	35.5(2.5) mJ/m^2
T-F NaCl	105(5) mJ/m^2
LJ	0.36(1) ϵ/σ^2
HS	0.58(3) k_BT/σ^2

VII. DISCUSSION

The results presented in this paper for mW water are somewhat different from those reported in Ref. 42. Here, we report a value for the ice-water interfacial free energy at coexistence of 35.5 ± 2.5 mN/m, whereas, in Ref. 42, we reported 29.5 ± 2.5 mN/m. Moreover, here we show in Fig. 5 that γ decreases as the supercooling increases, by contrast to Ref. 42 where we reported that γ changes little with temperature for the mW model. Consequently, the curves of J versus temperature reported here and in Ref. 42 are not the same. The main reason for the discrepancy with our previous work is that in Ref. 42 we used as starting configurations for the seeding study of mW those prepared for the TIP4P/2005 model. These models give similar densities for the fluid phase, but not quite for the solid phase. Therefore, in retrospect, borrowing configurations from the TIP4P/2005

model to study mW water was not a good idea. Moreover, we used the same order parameter as that used for TIP4P/2005 to determine the number of particles in the cluster. In the revisited calculations, we have tuned the order parameter specifically for the mW model as described in Section IV of this paper. With these improvements, our results for mW are more consistent than before: γ at coexistence coincides with that reported by Limmer and Chandler,[74] the extrapolation of J to high supercooling is consistent with previous calculations (see Fig. 3) and γ decreases as the supercooling increases, as observed for other water models.[42] Our mistake in the mW calculations highlights the importance of adequately generating the initial configuration in the seeding framework. We describe in detail how to generate initial configurations for seeding studies in Ref. 43.

In Fig. 3, we show that a seeding approach to crystal nucleation is successful in describing the nucleation rate for four different systems. It was unexpected to us that a simple theory like CNT was able to predict so well the nucleation rate up to very deep supercooling. In this work, our approach relies on the assumption that the critical clusters are spherical and have the structure of the equilibrium crystal phase, which is the simplest *a priori* description one can conceive for the nucleation mechanism. By using rare event techniques that do not impose any *a priori* mechanism, a more complex scenario may emerge for the structure of the critical nucleus.[13,14,37] Although from our results it seems that the correct nucleation rate can be obtained considering only spherical clusters with the equilibrium solid structure, this does not exclude that there are other independent nucleation pathways contributing to the rate. However, if there are not many alternative pathways and these are not faster than the path imposed in the seeding scheme, their contribution to the global nucleation rate would be within the error of the seeding method.

In any case, the seeding approach can also be used to calculate the nucleation rate for clusters with shapes other than spherical and structures different from that of the equilibrium crystal. For instance, in Ref. 66, we compare the ice nucleation rate via clusters with Ih and Ic structures and find that both paths have the same rate. Therefore, one can use the seeding approach to study the competition between freezing pathways going through any *a priori* conceivable critical cluster.

It should be added that the seeding method does not give information about the way the critical cluster is formed. Therefore, two-step mechanisms for the formation of the critical cluster[80–88] cannot be inferred from seeding, where a CNT-like growth pathway is implicity assumed. However, as long as the critical cluster structure is correctly guessed, one can use seeding to predict nucleation rates if sub-critical nuclei are in quasi-equilibrium with the fluid (the reversible work needed to go from the fluid to the fluid containing the critical cluster does not depend of the specific pathway by which such cluster is formed).

It is fair to mention again that our CNT fit captures virtually all the literature data within an error bar of four orders of magnitude. This may seem a large uncertainty but there are two considerations warranted in this respect. One is that discrepancies of 3 orders of magnitude can be found for the calculation of the nucleation rate via several more rigorous rare event techniques.[21] And the other is that we are estimating the nucleation rate in a range of hundreds of orders of magnitude, which is way larger than the afore mentioned uncertainty. Due to their computational cost, rigorous rare event techniques typically provide results in a range limited to tens of orders of magnitude.

Another aspect worth discussing is that it is in principle safer to apply the seeding technique to large clusters for two reasons. One is that a macroscopic theory like CNT is expected to work better in the limit of large clusters. Another is that the relative error in the number of particles in the cluster, N, decreases as the cluster size increases. This is because the determination of N relies on order parameters trained to identify bulk particles. Therefore, if there were a mistake in determining N it would be mainly due to a wrong labelling of surface particles. As the fraction of surface particles goes as $N^{-1/3}$, it is more convenient to use large clusters. Nonetheless, we have obtained reasonable nucleation rates using the seeding method for a cluster as small as ~300 particles in the HS system. In any case, from our experience we recommend to use the seeding technique for large N_c (>600 particles) and extrapolate the results to high supercooling with a CNT fit. With this procedure we have obtained nucleation rates consistent with the literature for the four models studied in this work.

VIII. CONCLUSIONS

These are the main conclusions we draw from our study of crystal nucleation via the seeding technique.

(i) Using the seeding method the nucleation rate can be computed at lower supercooling than with rigorous rare event techniques.
(ii) A fit to the seeding data based on Classical Nucleation Theory successfully compares to the data obtained at high supercooling with rigorous rare event methods. Such fit provides a reasonable estimate of the nucleation rate in a range of hundreds of orders of magnitude.
(iii) The extrapolation of the crystal-fluid interfacial free energy obtained from seeding to coexistence conditions is consistent with direct calculations of such quantity for all systems investigated.
(iv) These results suggest that, to a good approximation, one can describe crystal nucleation for the systems here investigated in the simplest way: the nucleation of a spherical critical cluster with the structure of the stable crystal.

ACKNOWLEDGMENTS

This work was funded by Grant No. FIS2013/43209-P of the MEC, UCM/Santander 910570, and by the Marie Curie Career Integration Grant No. 322326-COSAAC-FP7-PEOPLE-2012-CIG. C. Valeriani and E. Sanz acknowledge financial support from a Ramon y Cajal Fellowship. J. R. Espinosa acknowledges financial support from the FPI Grant No. BES-2014-067625. Calculations were carried

out in the supercomputer facility Tirant from the Spanish Supercomputing Network (RES) (Project No. QCM-2015-1-0028).

[1]K. F. Kelton, *Crystal Nucleation in Liquids and Glasses* (Academic, Boston, 1991).
[2]E. R. Buckle, "Studies on the freezing of pure liquids. II. The kinetics of homogeneous nucleation in supercooled liquids," Proc. R. Soc. A **261**(1305), 189–196 (1961).
[3]H. R. Pruppacher, "A new look at homogeneous ice nucleation in supercooled water drops," J. Atmos. Sci. **52**, 1924 (1995).
[4]B. J. Murray, S. L. Broadley, T. W. Wilson, S. J. Bull, R. H. Wills, H. K. Christenson, and E. J. Murray, "Kinetics of the homogeneous freezing of water," Phys. Chem. Chem. Phys. **12**, 10380 (2010).
[5]A. Manka, H. Pathak, S. Tanimura, J. Wolk, R. Strey, and B. E. Wyslouzil, "Freezing water in no man's land," Phys. Chem. Chem. Phys. **14**, 4505–4516 (2012).
[6]H. Laksmono, T. A. McQueen, J. A. Sellberg, N. D. Loh, C. Huang, D. Schlesinger, R. G. Sierra, C. Y. Hampton, D. Nordlund, M. Beye, A. V. Martin, A. Barty, M. M. Seibert, M. Messerschmidt, G. J. Williams, S. Boutet, K. Amann-Winkel, T. Loerting, L. G. M. Pettersson, M. J. Bogan, and A. Nilsson, "Anomalous behavior of the homogeneous ice nucleation rate in no-mans land," J. Phys. Chem. Lett. **6**(14), 2826–2832 (2015).
[7]L. Ickes, A. Welti, C. Hoose, and U. Lohmann, "Classical nucleation theory of homogeneous freezing of water: Thermodynamic and kinetic parameters," Phys. Chem. Chem. Phys. **17**, 5514–5537 (2015).
[8]P. N. Pusey and W. van Megen, "Phase behaviour of concentrated suspensions of nearly hard colloidal spheres," Nature **320**(27), 340 (1986).
[9]U. Gasser, E. R. Weeks, A. Schofield, P. N. Pusey, and D. A. Weitz, "Real-space imaging of nucleation and growth in colloidal crystallization," Science **292**, 258 (2001).
[10]S. C. Glotzer and M. J. Solomon, "Anisotropy of building blocks and their assembly into complex structures," Nat. Mater. **6**, 557–562 (2007).
[11]J. L. Harland and W. van Megen, "Crystallization kinetics of suspensions of hard colloidal spheres," Phys. Rev. E **55**, 3054 (1997).
[12]J. S. van Duijneveldt and D. Frenkel, "Computer simulation study of free energy barriers in crystal nucleation," J. Chem. Phys. **96**, 4655 (1992).
[13]P. R. ten Wolde, M. J. Ruiz-Montero, and D. Frenkel, "Numerical evidence for bcc ordering at the surface of a critical fcc nucleus," Phys. Rev. Lett. **75**, 2714 (1995).
[14]D. Moroni, P. R. ten Wolde, and P. G. Bolhuis, "Interplay between structure and size in a critical crystal nucleus," Phys. Rev. Lett. **94**, 235703 (2005).
[15]G. M. Torrie and J. P. Valleau, "Nonphysical sampling distributions in Monte Carlo free-energy estimation: Umbrella sampling," J. Comput. Phys. **23**, 187 (1977).
[16]A. Warmflash, P. Bhimalapuram, and A. R. Diner, "Umbrella Sampling for nonequilibrium processes," J. Chem. Phys. **127**, 154112 (2007).
[17]P. R. ten Wolde, M. J. Ruiz-Montero, and D. Frenkel, "Numerical calculation of the rate of crystal nucleation in a Lennard-Jones system at moderate undercooling," J. Chem. Phys. **104**, 9932 (1996).
[18]S. Auer and D. Frenkel, "Prediction of absolute crystal-nucleation rate in hard-sphere colloids," Nature **409**, 1020 (2001).
[19]R. Radhakrishnan and B. L. Trout, "Nucleation of hexagonal ice (I_h) in liquid water," J. Am. Chem. Soc. **125**, 7743 (2003).
[20]C. Valeriani, E. Sanz, and D. Frenkel, "Rate of homogeneous crystal nucleation in molten NaCl," J. Chem. Phys. **122**, 194501 (2005).
[21]L. Filion, M. Hermes, R. Ni, and M. Dijkstra, "Crystal nucleation of hard spheres using molecular dynamics, umbrella sampling, and forward flux sampling: A comparison of simulation techniques," J. Chem. Phys. **133**(24), 244115 (2010).
[22]A. Cuetos and M. Dijkstra, "Kinetic pathways for the isotropic–nematic phase transition in a system of colloidal hard rods: A simulation study," Phys. Rev. Lett. **98**, 095701 (2007).
[23]A. Reinhardt and J. P. K. Doye, "Free energy landscapes for homogeneous nucleation of ice for a monatomic water model," J. Chem. Phys. **136**(5), 054501 (2012).
[24]J. Russo, F. Romano, and H. Tanaka, "New metastable form of ice and its role in the homogeneous crystallization of water," Nat. Mater. **13**, 733 (2014).
[25]I. Saika-Voivod, F. Romano, and F. Sciortino, "Nucleation barriers in tetrahedral liquids spanning glassy and crystallizing regimes," J. Chem. Phys. **135**(12), 124506 (2011).
[26]C. Buhariwalla, R. Bowles, I. Saika-Voivod, F. Sciortino, and P. Poole, "Free energy of formation of small ice nuclei near the widom line in simulations of supercooled water," Eur. Phys. J. E **38**(5), 39 (2015).
[27]A. V. Brukhno, J. Anwar, R. Davidchack, and R. Handel, "Challenges in molecular simulation of homogeneous ice nucleation," J. Phys.: Condens. Matter **20**(49), 494243 (2008).
[28]P. Geiger and C. Dellago, "Neural networks for local structure detection in polymorphic systems," J. Chem. Phys. **139**(16), 164105 (2013).
[29]A. Haji-Akbari, R. S. DeFever, S. Sarupria, and P. G. Debenedetti, "Suppression of sub-surface freezing in free-standing thin films of a coarse-grained model of water," Phys. Chem. Chem. Phys. **16**, 25916–25927 (2014).
[30]R. J. Allen, P. B. Warren, and P. R. ten Wolde, "Sampling rare switching events in biochemical networks," Phys. Rev. Lett. **94**, 018104 (2005).
[31]E. Sanz, C. Valeriani, D. Frenkel, and M. Dijkstra, "Evidence for out-of-equilibrium crystal nucleation in suspensions of oppositely charged colloids," Phys. Rev. Lett. **99**, 055501 (2007).
[32]T. Li, D. Donadio, G. Russo, and G. Galli, "Homogeneous ice nucleation from supercooled water," Phys. Chem. Chem. Phys. **13**, 19807–19813 (2011).
[33]A. Haji-Akbari and P. G. Debenedetti, "Direct calculation of ice homogeneous nucleation rate for a molecular model of water," Proc. Natl. Acad. Sci. U. S. A. **112**(34), 10582–10588 (2015).
[34]A. Laio and M. Parrinello, "Escaping free-energy minima," Proc. Natl. Acad. Sci. U. S. A. **99**, 12562 (2002).
[35]F. Trudu, D. Donadio, and M. Parrinello, "Freezing of a Lennard-Jones fluid: From nucleation to spinodal regime," Phys. Rev. Lett. **97**, 105701 (2006).
[36]P. G. Bolhuis, D. Chandler, C. Dellago, and P. L. Geissler, "Transition path sampling: Throwing ropes over rough mountain passes, in the dark," Annu. Rev. Phys. Chem. **53**, 291 (2002).
[37]W. Lechner, C. Dellago, and P. G. Bolhuis, "Role of the prestructured surface cloud in crystal nucleation," Phys. Rev. Lett. **106**, 085701 (2011).
[38]X.-M. Bai and M. Li, "Calculation of solid-liquid interfacial free energy: A classical nucleation theory based approach," J. Chem. Phys. **124**(12), 124707 (2006).
[39]B. C. Knott, V. Molinero, M. F. Doherty, and B. Peters, "Homogeneous nucleation of methane hydrates: Unrealistic under realistic conditions," J. Am. Chem. Soc. **134**, 19544–19547 (2012).
[40]R. G. Pereyra, I. Szleifer, and M. A. Carignano, "Temperature dependence of ice critical nucleus size," J. Chem. Phys. **135**, 034508 (2011).
[41]E. Sanz, C. Vega, J. R. Espinosa, R. Caballero-Bernal, J. L. F. Abascal, and C. Valeriani, "Homogeneous ice nucleation at moderate supercooling from molecular simulation," J. Am. Chem. Soc. **135**(40), 15008–15017 (2013).
[42]J. R. Espinosa, E. Sanz, C. Valeriani, and C. Vega, "Homogeneous ice nucleation evaluated for several water models," J. Chem. Phys. **141**, 18C529 (2014).
[43]J. R. Espinosa, C. Vega, C. Valeriani, and E. Sanz, "The crystal-fluid interfacial free energy and nucleation rate of NaCl from different simulation methods," J. Chem. Phys. **142**(19), 194709 (2015).
[44]N. E. R. Zimmermann, B. Vorselaars, D. Quigley, and B. Peters, "Nucleation of NaCl from aqueous solution: Critical sizes, ion-attachment kinetics, and rates," J. Am. Chem. Soc. **137**(41), 13352 (2015).
[45]M. Volmer and A. Weber, Z. Phys. Chem. **119**, 277 (1926).
[46]R. Becker and W. Doring, Ann. Phys. **24**, 719–752 (1935).
[47]R. L. Davidchack and B. B. Laird, "Direct calculation of the crystal–melt interfacial free energies for continuous potentials: Application to the Lennard-Jones system," J. Chem. Phys. **118**(16), 7651–7657 (2003).
[48]J. R. Espinosa, C. Vega, and E. Sanz, "The mold integration method for the calculation of the crystal-fluid interfacial free energy from simulations," J. Chem. Phys. **141**(13), 134709 (2014).
[49]S. Angioletti-Uberti, M. Ceriotti, P. D. Lee, and M. W. Finnis, "Solid-liquid interface free energy through metadynamics simulations," Phys. Rev. B **81**, 125416 (2010).
[50]R. Benjamin and J. Horbach, "Crystal-liquid interfacial free energy via thermodynamic integration," J. Chem. Phys. **141**(4), 044715 (2014).
[51]V. Molinero and E. B. Moore, "Water modeled as an intermediate element between carbon and silicon," J. Phys. Chem. B **113**(13), 4008–4016 (2009).
[52]S. Plimpton, J. Comput. Phys. **117**, 1 (1995).
[53]J. Broughton and G. Gilmer, "Surface free energy and stress of a Lennard-Jones crystal," Acta Metall. **31**(6), 845–851 (1983).
[54]E. Lindahl, B. Hess, and D. van der Spoel, "Gromacs 3.0: A package for molecular simulation and trajectory analysis," J. Mol. Model. **7**, 306 (2001).
[55]J. Jover, A. J. Haslam, A. Galindo, G. Jackson, and E. A. Muller, "Pseudo hard-sphere potential for use in continuous molecular-dynamics simulation of spherical and chain molecules," J. Chem. Phys. **137**(14), 144505 (2012).
[56]J. R. Espinosa, E. Sanz, C. Valeriani, and C. Vega, "On fluid–solid direct coexistence simulations: The pseudo-hard sphere model," J. Chem. Phys. **139**(14), 144502 (2013).

[57]F. Fumi and M. Tosi, "Ionic sizes and born repulsive parameters in the NaCl-type alkali halides. I," J. Phys. Chem. Solids **25**, 31–43 (1964).
[58]M. Tosi and F. Fumi, "Ionic sizes and born repulsive parameters in the NaCl-type alkali halides. II," J. Phys. Chem. Solids **25**, 45–52 (1964).
[59]J. L. Aragones, E. Sanz, C. Valeriani, and C. Vega, "Calculation of the melting point of alkali halides by means of computer simulations," J. Chem. Phys. **137**(10), 104507 (2012).
[60]U. Essmann, L. Perera, M. L. Berkowitz, T. Harden, H. Lee, and L. G. Pedersen, "A smooth particle mesh Ewald method," J. Chem. Phys. **103**, 8577 (1995).
[61]M. Parrinello and A. Rahman, "Polymorphic transitions in single crystals: A new molecular dynamics method," J. Appl. Phys. **52**, 7182–7190 (1981).
[62]G. Bussi, D. Donadio, and M. Parrinello, "Canonical sampling through velocity rescaling," J. Chem. Phys. **126**(1), 014101 (2007).
[63]W. G. Hoover, "Canonical dynamics: Equilibrium phase-space distributions," Phys. Rev. A **31**, 1695 (1985).
[64]W. G. Hoover, "Constant-pressure equations of motion," Phys. Rev. A **34**, 2499–2500 (1986).
[65]S. Melchionna, G. Ciccotti, and B. L. Holian, "Hoover NPT dynamics for systems varying in shape and size," Mol. Phys. **78**(3), 533–544 (1993).
[66]A. Zaragoza, M. M. Conde, J. R. Espinosa, C. Valeriani, C. Vega, and E. Sanz, "Competition between ices Ih and Ic in homogeneous water freezing," J. Chem. Phys. **143**(13), 134504 (2015).
[67]J. Benet, L. G. MacDowell, and E. Sanz, "Computer simulation study of surface wave dynamics at the crystal-melt interface," J. Chem. Phys. **141**(3), 034701 (2014).
[68]J. Benet, L. G. MacDowell, and E. Sanz, "A study of the ice-water interface using the TIP4P/2005 water model," Phys. Chem. Chem. Phys. **16**, 22159–22166 (2014).
[69]S. Auer and D. Frenkel, "Numerical prediction of absolute crystallization rates in hard-sphere colloids," J. Chem. Phys. **120**, 3015 (2004).
[70]W. Lechner and C. Dellago, "Accurate determination of crystal structures based on averaged local bond order parameters," J. Chem. Phys. **129**(11), 114707 (2008).
[71]E. B. Moore and V. Molinero, "Structural transformation in supercooled water controls the crystallization rate of ice," Nature **479**(7374), 506–508 (2011).
[72]J. J. Hoyt, M. Asta, and A. Karma, "Method for computing the anisotropy of the solid–liquid interfacial free energy," Phys. Rev. Lett. **86**, 5530–5533 (2001).
[73]J. Q. Broughton and G. H. Gilmer, "Molecular dynamics investigation of the crystal–fluid interface. VI. Excess surface free energies of crystal–liquid systems," J. Chem. Phys. **84**(10), 5759–5768 (1986).
[74]D. T. Limmer and D. Chandler, "Phase diagram of supercooled water confined to hydrophilic nanopores," J. Chem. Phys. **137**(4), 044509 (2012).
[75]J. R. Morris and X. Song, "The anisotropic free energy of the Lennard-Jones crystal-melt interface," J. Chem. Phys. **119**, 3920 (2003).
[76]R. L. Davidchack, J. R. Morris, and B. B. Laird, "The anisotropic hard-sphere crystal-melt interfacial free energy from fluctuations," J. Chem. Phys. **125**, 094710 (2006).
[77]R. L. Davidchack, "Hard spheres revisited: Accurate calculation of the solid–liquid interfacial free energy," J. Chem. Phys. **133**(23), 234701 (2010).
[78]R. Benjamin and J. Horbach, "Crystal-liquid interfacial free energy of hard spheres via a thermodynamic integration scheme," Phys. Rev. E **91**, 032410 (2015).
[79]A. Härtel, M. Oettel, R. E. Rozas, S. U. Egelhaaf, J. Horbach, and H. Löwen, "Tension and stiffness of the hard sphere crystal-fluid interface," Phys. Rev. Lett. **108**, 226101 (2012).
[80]P. R. ten Wolde and D. Frenkel, "Enhancement of protein crystal nucleation by critical density fluctuations," Science **277**, 1975 (1997).
[81]B. OMalley and I. Snook, "Structure of hard-sphere fluid and precursor structures to crystallization," J. Chem. Phys. **123**(5), 054511 (2005).
[82]H. J. Schöpe, G. Bryant, and W. van Megen, "Two-step crystallization kinetics in colloidal hard-sphere systems," Phys. Rev. Lett. **96**, 175701 (2006).
[83]T. Kawasaki and H. Tanaka, "Formation of a crystal nucleus from liquid," Proc. Natl. Acad. Sci. U. S. A. **107**(32), 14036–14041 (2010).
[84]T. Schilling, H. J. Schöpe, M. Oettel, G. Opletal, and I. Snook, "Precursor-mediated crystallization process in suspensions of hard spheres," Phys. Rev. Lett. **105**, 025701 (2010).
[85]Y. C. Shen and D. W. Oxtoby, "Nucleation of Lennar-Jones fluids: A density functional approach," J. Chem. Phys. **105**(15), 6517–6524 (1996).
[86]J. F. Lutsko and G. Nicolis, "Theoretical evidence for a dense fluid precursor to crystallization," Phys. Rev. Lett. **96**, 046102 (2006).
[87]T. Kawasaki and H. Tanaka, "Structural origin of dynamic heterogeneity in three-dimensional colloidal glass formers and its link to crystal nucleation," J. Phys.: Condens. Matter **22**(23), 232102 (2010).
[88]J. Russo and H. Tanaka, "The microscopic pathway to crystallization in supercooled liquids," Sci. Rep. **2**, 505 (2012).